SCIEPublish

Article

Exploring the Potential Relationship between Gut Microbiome Metabolites and Idiopathic Pulmonary Fibrosis via Network Pharmacology Study

Zhenwei Li, Zhao Zhu, Jiawei Wang, Mengke Zhang, Yulong Gan, Yinan Yan and Lan Wang *

State Key Laboratory of Cell Differentiation and Regulation, Henan International Joint Laboratory of Pulmonary Fibrosis, Henan Center for Outstanding Overseas 8, Henan Normal University, Xinxiang 453007, China; 2204183024@stu.htu.edu.cn (Z.L.); 2204283154@stu.htu.edu.cn (Z.Z.); 2204183081@stu.htu.edu.cn (J.W.); 2304183027@stu.htu.edu.cn (M.Z.); 2304183086@stu.htu.edu.cn (Y.G.); 2304283133@stu.htu.edu.cn (Y.Y.)

* Corresponding author. E-mail: wanglan@htu.edu.cn (L.W.); Tel.: +86-373-3326340 (L.W.)

Received: 29 September 2024; Revised: 3 October 2024; Accepted: 28 October 2024; Available online: 4 November 2024

ABSTRACT: Idiopathic pulmonary fibrosis (IPF) is a chronic, progressive fibrotic lung disease with a poor prognosis. Previous research has revealed that the gut microbiota is associated with human health and immunity, and it interacts with the lung through the "gut-lung axis". This study explores the potential relationship between Gut Microbiome Metabolites and Idiopathic pulmonary fibrosis via Network Pharmacology Study. The metabolites from gut microbiota were retrieved from the gutMGene database, and gene targets for these metabolites were obtained from previous studies. Gene targets of IPF were obtained from public databases (DisGeNET, OMIM). Subsequently, following the identification of shared targets, IL6 was determined as the core target through protein-protein interaction analysis. Then, a microbiota-metabolite-target-signaling pathway network (MMTS) was constructed using Cytoscape 3.10, and targets with low expression in the lungs and intestines were deleted. The MMTS network revealed that three short-chain fatty acids—acetate, butyrate, propionate, and a flavonoid compound called equol—are IL6-related metabolites. Then, we performed a molecular docking test (MDT) using CB-Dock2 to validate the affinity between core targets and metabolites. MDT confirmed that equol produced by the conversion of isoflavones from *Lactobacillus paracasei* JS1 was more stable in binding to IL6 than the other three short-chain fatty acids, thereby affecting multiple signaling pathways and influencing the progression of IPF. Finally, we validated this hypothesis through *in vitro* cell culture experiments, further confirming the effect of Equol.

Keywords: Idiopathic Pulmonary Fibrosis; Network pharmacology; Equol; Gut microbiota

1. Introduction

Idiopathic pulmonary fibrosis (IPF) is a chronic, progressive pulmonary disease characterized by persistent pulmonary scarring, usually histologically presenting as interstitial pneumonia (UIP) [1,2]. As the disease advances, healthy lung tissue undergoes gradual replacement by an altered extracellular matrix, destroying the alveolar structure. This leads to decreased lung compliance, impairing gas exchange, and ultimately culminating in respiratory failure and mortality. Presently, treatment options for IPF remain limited, with diagnosed patients having a median survival time of only 3–5 years. Strategies aimed at delaying or even reversing the progression of IPF represent a pivotal and challenging area of investigation in this field [3].

Damage, aberrant senescence, ref. [4] and apoptosis of alveolar epithelial cells (AECs), as well as dysfunctional repair after injury leading to tissue fibrotic changes, are regarded as the core pathogenesis of IPF [5–7]. Among them, disorders of immune regulation play an important role in the pathogenesis of IPF [8,9]. IL-6 (Interleukin-6) is a pivotal cytokine involved in immune regulation and inflammation. It stimulates immune cells such as T, B, and NK cells, enhancing their proliferation and activity. In pulmonary fibrosis, IL-6 plays a crucial role by promoting inflammation, activating fibroblasts to produce collagen and other extracellular matrix components, increasing the production of tissue inhibitors of metalloproteinases (TIMPs) to inhibit collagen breakdown, and influencing immune regulation within the lungs [10–12].

https://doi.org/10.70322/fibrosis.2024.10009

In recent years, research on the interaction between microbiota and hosts has gradually emerged as an important avenue for understanding various diseases [13], with particular attention given to the role of gut microbiota.

There is a complex microbial ecosystem in the intestinal tract. This ecosystem profoundly influences the host's immune, metabolic, and overall physiological health. Metabolites generated by the intestinal microbiota regulate the host's physiological processes [14]. These metabolites play critical roles in energy metabolism and exert profound effects on the host's inflammatory responses through modulation of the immune system. Changes in the gut microbiota and its metabolites can activate various immune and non-immune cells in the host, inducing inflammatory responses and triggering the production of abundant extracellular matrix (ECM) components by mesenchymal cells [15]. This common pathogenic factor leads to fibrotic lesions in other extraintestinal organs [16]. Although the pathogenic mechanisms of idiopathic pulmonary fibrosis (IPF) are not yet fully understood, substantial evidence indicates an association with immune-inflammatory damage [17]. Therefore, in the context of IPF, researchers have begun to explore the potential roles of gut microbiota and their metabolites in disease progression.

Lactobacillus paracasei JS1 is a lactobacillus that metabolizes soy isoflavones in the human gastrointestinal tract to produce equol in the gut. It has a better anti-inflammatory effect than daidzein [18]. Previous studies have identified significant differences in the gut microbiota and metabolites between control groups and two mouse models of pulmonary fibrosis induced by bleomycin and silica dust [19]. Studies have found that Lactobacillus, as a probiotic, significantly reduced fibrosis in a bleomycin-induced pulmonary fibrosis model [20,21]. *Lactobacillus paracasei* JS1 may be altered in patients with pulmonary fibrosis.

Previous studies have shown that equinestrol can reduce LPS-induced NO production, thereby reducing the neuroinflammation of LPS-activated mouse glial cells [22], and can affect multiple signaling pathways and reduce the expression of pro-inflammatory cytokines (IL-6 and TNF-α) [23]. At the same time, equol administration inhibited the expression of IL-6 and its receptor in the inflamed region of collagen-induced arthritis mice [24]. However, the role of equol in IPF is unknown.

In our study, we found that equol, a metabolite produced by *Lactobacillus paracasei* JS1, may influence the target IL6 in pulmonary fibrosis through the microbiota-metabolite-target signaling pathway network (MMTS).

This study offers new evidence for the interplay between the gut and lungs in fibrotic lung diseases.

By delving into the intricate relationship between gut microbiota and IPF, we stand to gain a more comprehensive understanding of the disease's progression, paving the way for more precise and innovative treatment approaches in the future [25]. With a deeper understanding of the interactions between gut microbiota and IPF, we can anticipate clearer and more forward-thinking directions for future research and therapeutic interventions.

2. Materials and Methods

2.1. Study Design

In this study, we utilized various online biological databases to conduct queries and obtain rich data on microbiota, metabolites, disease genes, and related aspects. We integrated and filtered crucial information by selecting appropriate databases, providing vital support for our research questions. Through data analysis, we delved deeper into the structure and function of biological systems, driving the progress of our research. Throughout the study, we placed high importance on the reliability and consistency of the data, striving to integrate our research findings with existing literature to form a more comprehensive and in-depth research perspective. The databases used are summarized in Table 1.

Table 1. All the databases used.

No.	Databases	Utilization	URL
1	gutMGene	The retrieval of targets and metabolites of gut microbes	http://bio-annotation.cn/gutmgene (accessed on 1 December 2023)
2	SwissTargetPrediction	To search for metabolite targets of intestinal microbes	http://www.swisstargetprediction.ch/ (accessed on 1 December 2023)
3	Similarity ensemble approach	To search for metabolite targets of intestinal microbes	https://sea.bkslab.org/ (accessed on 1 December 2023)
4	DisGeNET	The pioneering of targets responded to diseases	https://www.disgenet.org/ (accessed on 1 December 2023)
5	Online Mendelian Inheritance in Man (OMIM)	The correlation of human targets and diseases	https://www.omim.org/ (accessed on 1 December 2023)
6	Venny2.1	Draw VENN diagram	https://bioinfogp.cnb.csic.es/tools/venny/ (accessed on 1 December 2023)
7	String	Protein interaction network analysis was performed	https://string-db.org/ (accessed on 1 December 2023)
8	The Human Protein Atlas	Look at the expression of the target in the lung and gastrointestinal tract	https://www.proteinatlas.org/ (accessed on 3 December 2023)
9	RCSB Protein Data Bank	Download protein 3d structures for molecular docking	https://www.rcsb.org/ (accessed on 3 December 2023)
10	PubChem	Download 3d structures of compounds for molecular docking	https://pubchem.ncbi.nlm.nih.gov/ (accessed on 3 December 2023)
11	CB-Dock2	Conduct molecular docking experiments	https://cadd.labshare.cn/cb-dock2/php/index.php (accessed on 3 December 2023)
12	SwissADME	The identification of physicochemical properties on compounds	http://www.swissadme.ch/ (accessed on 3 December 2023)

First, we accessed gutMGene (accessed on 1 December 2023) to obtain metabolites produced by the gut microbiota and their respective target substrates. It is important to note that the gutMGene database is limited to gut-derived metabolites and does not include information on microbiomes associated with lung fibrotic diseases such as idiopathic pulmonary fibrosis (IPF). The targets of metabolites were derived from previous research [26]. IPF targets were determined using DisGeNET (accessed on 1 December 2023) and OMIM (visited on 1 December 2023) [27,28]. A protein-protein interaction (PPI) network was constructed to identify interactions between each node. Subsequently, gene expression levels in lung tissue and gastrointestinal tissue were queried. Genes with average expression levels below 1 Transcripts Per Kilobase per Million mapped reads (TPM) were excluded when constructing the MMTS network. The MMTS network was built using Cytoscape 3.10, and a metabolic network of core targets was constructed. Following this, the stability of binding between metabolites and targets was evaluated using MDT. Then, we validated whether Equol could affect IL6 expression through *in vitro* experiments using qPCR and Western blot (WB) analysis.

2.1.1. Obtain Metabolites and Their Target Substrates from the Gut Microbiota

Data on metabolites and their corresponding targets within the gut microbiota were sourced from gutMGene (http://bio-annotation.cn/gutmgene (accessed on 1 December 2023)). Detailed information regarding the human gut microbiota, its metabolites, and associated targets was acquired through the download section of gutMGene v1.0 (http://bioannotation.cn/gutmgene/public/res/gutMGene-human.xlsx (accessed on 1 December 2023)) Supplementary Table S1.

2.1.2. Acquisition of Metabolite Targets and Disease Targets

The metabolite targets used in this study were sourced from previous research, with the article providing information on the overlapping targets of gut microbiota metabolites from the SEA and STP databases. Venn diagrams were generated using Venny 2.1.0 to illustrate the overlap of targets between gut microbiota metabolites from the SEA and STP databases. IPF disease target data were obtained from DisGeNET (https://www.disgenet.org/ (accessed on 1 December 2023)) and OMIM (https://www.omim.org/ (accessed on 1 December 2023)), with DisGeNET and OMIM serving as disease-target association databases. A keyword search for “Idiopathic Pulmonary Fibrosis” was conducted, and the deduplicated summary yielded relevant targets associated with IPF.

2.1.3. Identification of Targets Related to IPF

Plot the overlap between gut microbiota targets and IPF. Then, create a Venn diagram of these overlapping targets and targets from the gutMGene database identified in the previous step. We consider these targets to be core targets within the gut microbiota that influence IPF.

2.1.4. Construction of Protein-Protein Interaction (PPI) Network

Using the STRING database (https://string-db.org/ (accessed on 1 December 2023)), analyze the core targets obtained in Step 3. Construct a protein-protein interaction (PPI) network of the core targets, selecting interactions with a comprehensive score > 0.9. After removing targets that do not form a network, export the PPI data as a tsv file, and import it into Cytoscape software for network visualization. Through the analysis of the PPI protein interaction network, core genes influencing IPF are identified based on network connectivity.

2.1.5. Enrichment Analysis of GO and KEGG Pathways

To gain deeper insights into the functions and regulatory mechanisms of core targets within cells, we imported the identified core genes into the R environment. We analyzed Gene Ontology (GO) and Kyoto Encyclopedia of Genes and Genomes (KEGG) pathway using the clusterProfiler package. GO analysis included molecular functions (MF), biological processes (BP), and cellular components (CC). Simultaneously, we visualized the enrichment analysis results using the ggplot2 package, with GO analysis results presented as bar plots and KEGG analysis results displayed as bubble plots. Ultimately, these visualizations enhanced our understanding of the functions and regulatory mechanisms of the core targets.

2.1.6. Expression of Key Genes in the Lungs and Gastrointestinal Tract

To gather expression data for key targets in normal lung and gastrointestinal tissues, we utilized resources from The Human Protein Atlas website. Using data visualization in R, we aimed to develop a comprehensive view of these targets' expression patterns across tissues under physiological conditions. In the subsequent construction of the MMTS network, genes with an average expression level below 1 TPM were excluded to ensure the reliability and accuracy of the analysis results.

2.1.7. Construction of a Microbiome-Signaling Pathway Target-Metabolite Network

Constructing a Microbiota-Metabolite-Target- signaling Pathway network using Cytoscape, filtering microbiota and metabolites directly associated with the targets from the gutMgene database. Microbiota, signaling pathways, targets, and metabolites are represented as nodes in the network, filtering out metabolite-target pairs that lack connections.

2.1.8. Molecular Docking Experiment

Perform a secondary screening of metabolites affecting IL6 based on the threshold of metabolites related to the core target with a Gibbs free energy of <−6.0 kcal/mol or the lowest Gibbs free energy (most negative value).

Download the 3D structure of the protein from RCSB (https://www.rcsb.org/ (accessed on 3 December 2023)) (accessed on 1 December 2023). Process the extracted .pdb format files from RCSB using pdbtools (PDB Tools (labshare.cn)) for hydrogenation. Download the 3D structure of the ligand from PubMed. CB-Dock2 (https://cadd.labshare.cn/cb-dock2/index.php (accessed on 3 December 2023)) is a protein-ligand docking tool based on AutoDock Vina. Conduct protein-ligand docking predictions and visualization using CB-Dock2.

2.2. Experimental Verification In Vitro

2.2.1. Cells and Reagents

Human monocytes (THP-1) were purchased from the American Type Culture Collection (ATCC), and Equol (purity 99.25%, HY-100583A) was obtained from MCE. Lipopolysaccharide (LPS) from *Escherichia coli* was purchased from List Labs, and DMSO was obtained from Fangzheng Reagent in Beichen District, Tianjin. Fetal bovine serum (FBS) was purchased from Excell, and Roswell Park Memorial Institute-1640 (RPMI-1640) medium was obtained from Cytiva (UK). IL6 and β-actin antibodies were provided by Beijing Biosynthesis Biotechnology. Goat anti-rabbit IgG and goat anti-mouse IgG were purchased from Abcam. The Cell Counting Kit-8 (CCK8) was obtained

from Beyotime. PCR primers were synthesized by Sangon (ShangHai, China). All primer sequences are shown in the primer table (Table 2).

Table 2. PCR primers.

ACTB-Forward Sequence	CACCATTGGCAATGAGCGGTTC
Reverse Sequence	AGGTCTTTGCGGATGTCCACGT
IL6-Forward Sequence	AGACAGCCACTCACCTCTTCAG
Reverse Sequence	TTCTGCCAGTGCCTCTTTGCTG

2.2.2. RT-qPCR Analysis

THP-1 cells were differentiated with PMA for 12 h, followed by treatment with LPS (100 ng/mL) containing different concentrations of Equol for 8 h. Total RNA was then extracted from the cells using Trizol. The concentration of total RNA was measured using a NanoDrop One spectrophotometer (Thermo Scientific, Waltham, MA, USA). Total RNA was reverse transcribed into cDNA using the HiFiScript gDNA Removal cDNA Synthesis Kit. The PCR reactions were prepared using the SYBR Green PCR Master Mix (Low ROX) kit to amplify the cDNA, and expression levels were detected using the Roche LightCycler 480 (Roche Diagnostics, Basel, Switzerland). The relative expression of the target gene was calculated using the $2^{-\Delta\Delta Ct}$ method.

2.2.3. Western Blot Analysis

THP-1 cells were differentiated with PMA for 12 h, and after the cells adhered, they were cultured with LPS and LPS-containing media with different concentrations of Equol for 8 h. The cells were washed with 1X phosphate-buffered saline (PBS), and cell proteins were extracted using SDS lysis buffer. Protein concentrations were measured and separated by 10% SDS-polyacrylamide gel electrophoresis (SDS-PAGE). The proteins were then transferred onto polyvinylidene fluoride (PVDF) membranes (Millipore, Billerica, MA, USA) and blocked with TBST containing 5% non-fat milk. The target proteins were incubated overnight at 4 °C with the specific primary antibodies. The following day, after washing off the excess primary antibodies with TBST, the membranes were incubated with secondary antibodies at room temperature for 1 h, and protein bands were visualized using a gel imaging system.

The whole research process is shown in Figure 1.

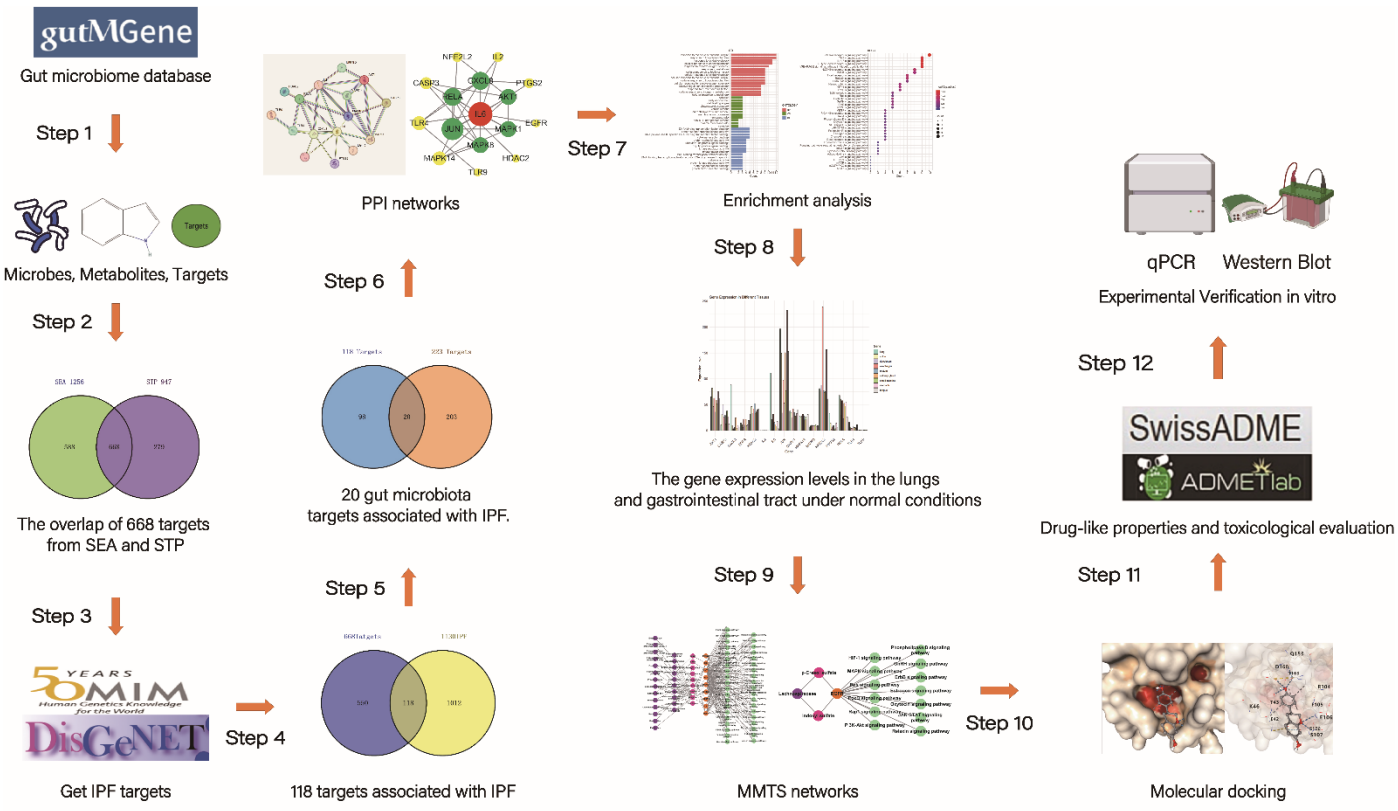

Figure 1. The analysis process of the whole work.

2.2.4. Statistical Analysis

All values are expressed as mean ± SEM. One-way ANOVA (Dunnett's *t*-test) was used, and $p < 0.05$ was considered statistically significant.

Our observational study suggests that Lactobacillus JS1, as a probiotic, can metabolize to produce Equol, which can influence IL6 and thereby affect IPF.

3. Results

3.1. The Results of Getting Targets

From the gutMGene database, a total of 208 metabolites were obtained. The targets of these metabolites were extracted from the article, resulting in 1256 from the SEA source and 947 from the STP source. An overlap of 668 targets was observed between SEA and STP sources (Figure 2A). Venn diagram analysis revealed 118 common targets between the 668 targets and the targets related to IPF (1130 targets) (Figure 2B).

Finally, from the 223 targets obtained from the gutMGene database, we selected 20 core targets overlapping with the 118 targets for protein-protein interaction (PPI) network analysis (Supplementary Table S2, Figure 2C).

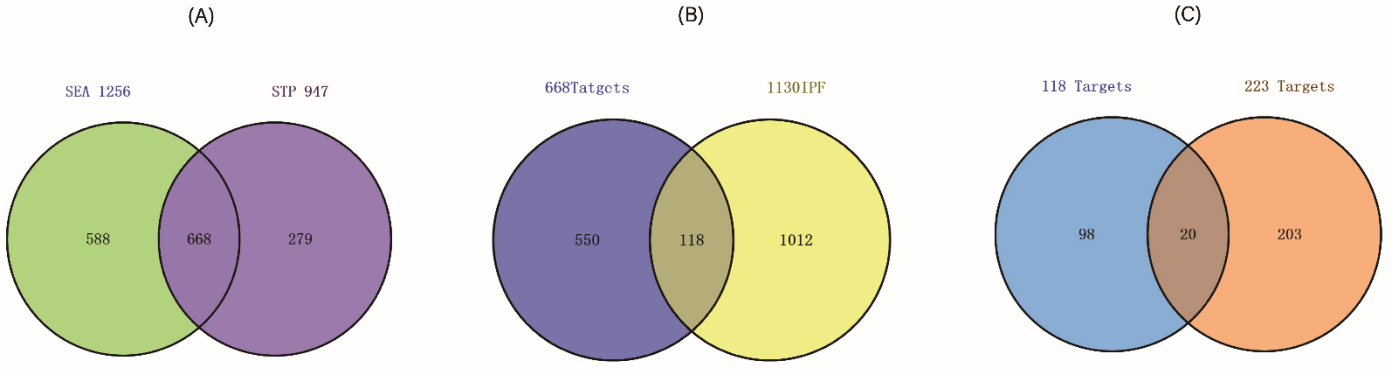

Figure 2. (**A**) The number of overlapping 668 targets between SEA (1256 targets) and STP (947 targets). (**B**) The number of overlapping 118 targets between the 668 targets and IPF targets (1130 targets). (**C**) The final overlapping of 20 targets between the 118 and gut human targets (223 targets).

3.2. PPI Network

The PPI network consisted of 16 nodes and 32 edges. Notably, HDAC7, HDAC8, HDAC9, and HPGD showed no interactions with other targets in the PPI network. The highest degree of centrality in the PPI network was observed for IL6, followed by JUN, RELA, and CXCL8 (Figure 3A,B, Table 3).

Table 3. The degree of targets on the PPI network.

Number	Gene Name	Degree
1	*IL6*	9
2	*JUN*	8
3	*CXCL8*	6
4	*RELA*	6
5	*AKT1*	5
6	*MAPK1*	5
7	*MAPK8*	5
8	*MAPK14*	4
9	*TLR4*	4
10	*CASP3*	3
11	*NFE2L2*	2
12	*IL2*	2
13	*PTGS2*	2
14	*EGFR*	1
15	*HDAC2*	1
16	*TLR9*	1

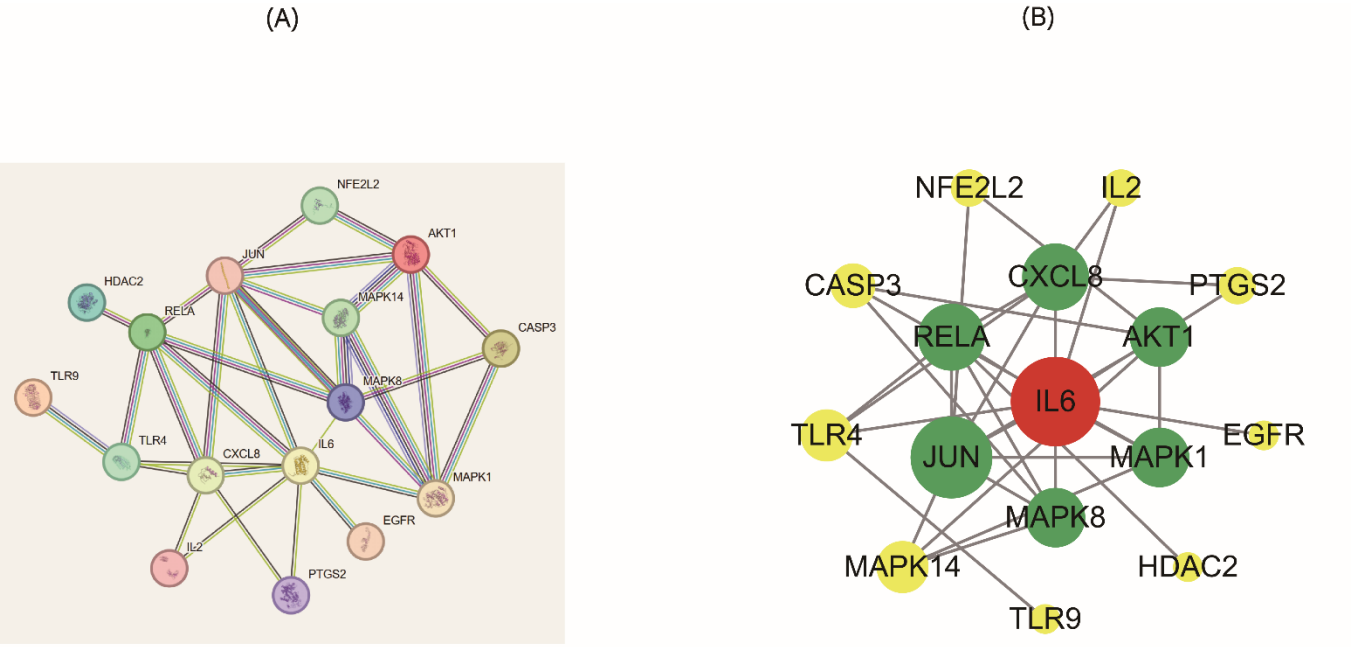

Figure 3. Protein-Protein Interaction Networks. (**A**) PPI network from STRING. (**B**) PPI network from Cytoscape.

3.3. Enrichment Analysis

GO term enrichment analysis mainly contains cellular components (CC), biological processes (BP), and molecular functions (MF).

We mainly chose the results of KEGG. The enrichment analysis results indicate that 16 core targets are directly associated with 40 signaling pathways in IPF. Among these pathways, the AGE-RAGE signaling pathway in diabetic complications, TNF signaling pathway, IL-17 signaling pathway, and Toll-like receptor signaling pathway are likely crucial pathways influencing IPF. (Figure 4B, Table 4).

Table 4. Signaling pathways associated with IPF.

ID	Description	ID	p.adjust	Count
hsa04933	AGE-RAGE signaling pathway in diabetic complications	IL6/TNF/IL1B/CXCL8/TGFB1/NFKB1/AKT1/CCL2/IL1A /BCL2/JUN/CASP3	2.16×10^{-18}	12
hsa04657	IL-17 signaling pathway	IL6/TNF/IL1B/IFNG/CXCL8/NFKB1/CCL2/PTGS2/JUN/ CASP3/IL4	8.71×10^{-17}	11
hsa04620	Toll-like receptor signaling pathway	IL6/TNF/IL1B/CXCL8/NFKB1/AKT1/TLR4/JUN/TLR2	2.05×10^{-12}	9
hsa04668	TNF signaling pathway	IL6/TNF/IL1B/NFKB1/AKT1/CCL2/PTGS2/JUN/CASP3	3.11×10^{-12}	9
hsa04625	C-type lectin receptor signaling pathway	IL6/TNF/IL1B/NFKB1/AKT1/PTGS2/IL10/JUN	9.73×10^{-11}	8
hsa04621	NOD-like receptor signaling pathway	IL6/TNF/IL1B/CXCL8/NFKB1/CCL2/BCL2/TLR4/JUN	2.36×10^{-10}	9
hsa04064	NF-kappa B signaling pathway	TNF/IL1B/CXCL8/NFKB1/PTGS2/BCL2/TLR4	4.79×10^{-9}	7
hsa04659	Th17 cell differentiation	IL6/IL1B/IFNG/TGFB1/NFKB1/JUN/IL4	6.05×10^{-9}	7
hsa05130	Pathogenic *Escherichia coli* infection	IL6/TNF/IL1B/CXCL8/NFKB1/TLR4/JUN/CASP3	1.25×10^{-8}	8
hsa04660	T cell receptor signaling pathway	TNF/IFNG/NFKB1/AKT1/IL10/JUN/IL4	1.27×10^{-8}	7
hsa05235	PD-L1 expression and PD-1 checkpoint pathway in cancer	IFNG/NFKB1/AKT1/TLR4/JUN/TLR2	7.51×10^{-8}	6
hsa04066	HIF-1 signaling pathway	IL6/IFNG/NFKB1/AKT1/BCL2/TLR4	2.43×10^{-7}	6
hsa04010	MAPK signaling pathway	TNF/IL1B/TGFB1/NFKB1/AKT1/IL1A/JUN/CASP3	2.62×10^{-7}	8
hsa04630	JAK-STAT signaling pathway	IL6/IFNG/AKT1/BCL2/IL10/IL4	2.42×10^{-6}	6
hsa05022	Pathways of neurodegeneration-multiple diseases	IL6/TNF/IL1B/NFKB1/IL1A/PTGS2/BCL2/CASP3	6.57×10^{-6}	8
hsa04672	Intestinal immune network for IgA production	IL6/TGFB1/IL10/IL4	7.80×10^{-6}	4
hsa04151	PI3K-Akt signaling pathway	IL6/NFKB1/AKT1/BCL2/TLR4/IL4/TLR2	1.23×10^{-5}	7

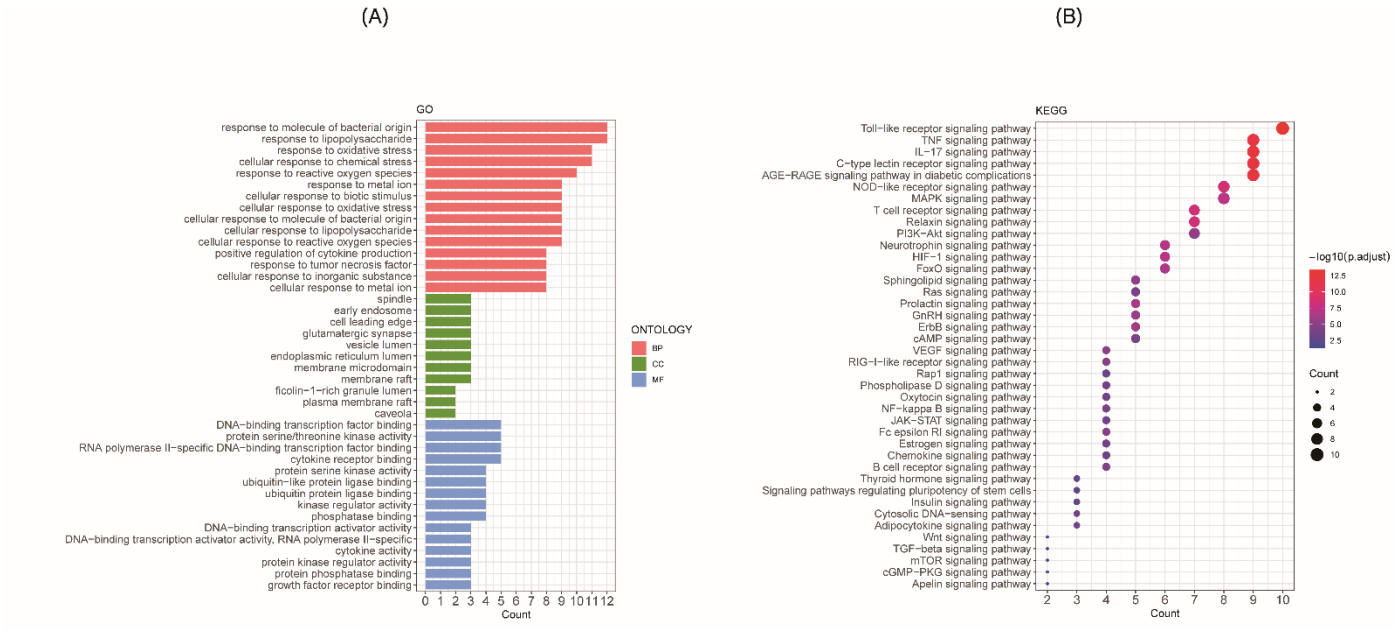

Figure 4. Enrichment analysis. (**A**) GO enrichment analysis results. (**B**) KEGG enrichment analysis results.

3.4. Expression Levels of the Targets

Subsequently, expression levels of the targets in the gastrointestinal tract and lungs were queried. Among these, the average expression levels of IL2 and TLR9 were lower than 1 TPM. Therefore, during the construction of the MMTS network, IL2 and TLR 9 were ignored (Figure 5).

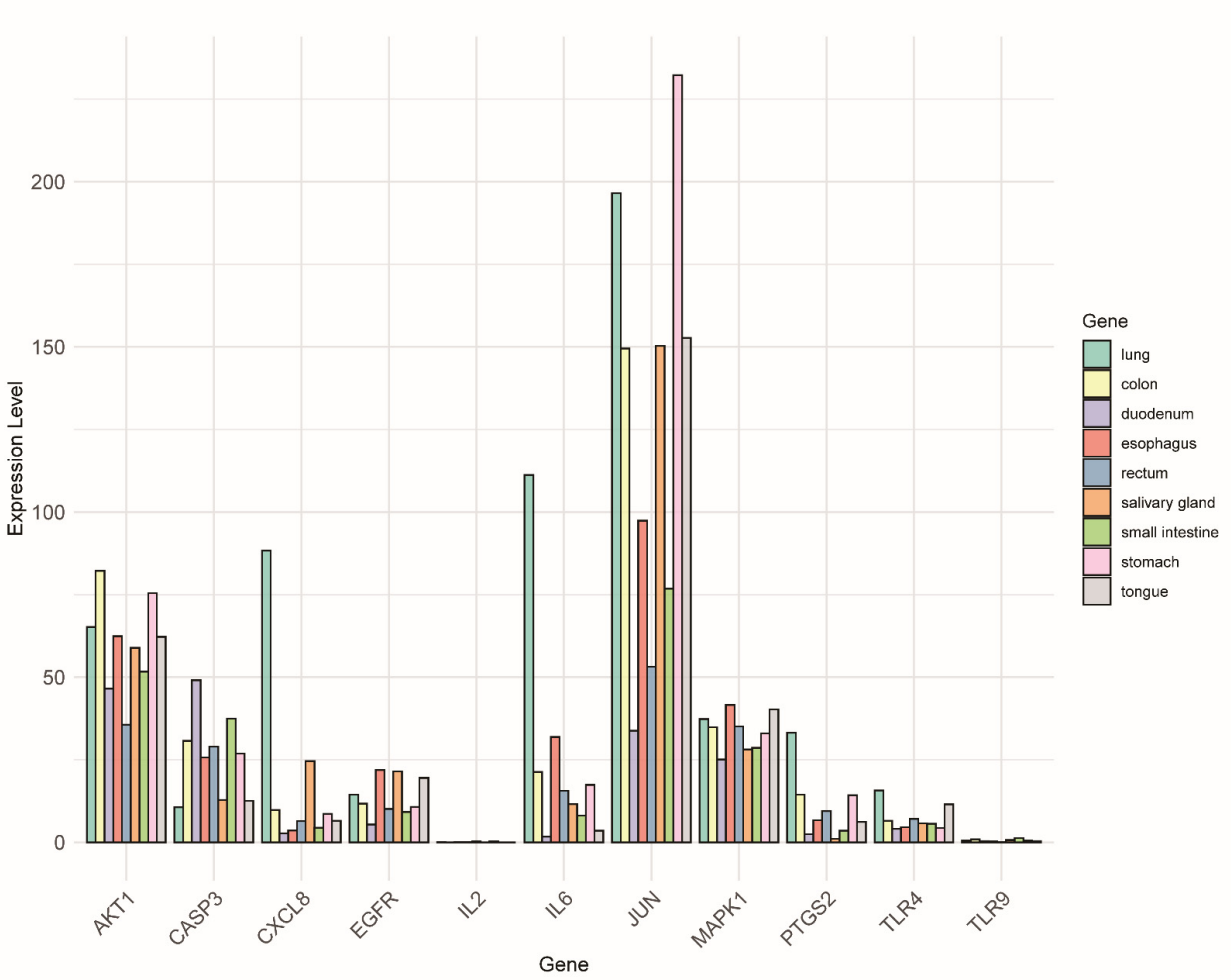

Figure 5. Gene Expression in Different Tissues.

3.5. MMTS Network and Molecular Docking

The MMTS network illustrates the relationships among microbiota, signaling pathways, targets, and metabolites. After filtering out unconnected nodes and genes with insignificant expression, a network comprising 82 nodes (including 24 microbiota, 40 signaling pathways, 11 targets, and 9 metabolites) and 172 edges were formed (Figure 6A).

Subsequently, a MMTS network for the core target IL6 (PDB ID: 1alu) was constructed (Figure 6B). It was observed that three short-chain fatty acids (Acetate, Butyrate, Propionate) and one flavonoid compound (Equol) could influence IL6. In molecular docking experiments, Acetate, Butyrate, Propionate, and IL6 binding energies were −3.0, −3.7, and −3.4 kcal/mol. The Equol had a binding energy of −6.1 kJ/mol with IL6. At the same time, the binding energies of Acetate, Butyrate, Propionate, and IL6-R were −3.0, −4.3, and −3.6 kcal/mol. The Equol had a binding energy of −6.7 kJ/mol with IL6-R(Figure 7A). Given the relatively low binding energies of short-chain fatty acids with IL6 and IL6-R, emphasis was placed on the action of Equol (Figure 7B). Based on the screening criterion of binding energy ≤ −5.0 kcal/mol, Equol demonstrated superior binding potential compared to the other three compounds.

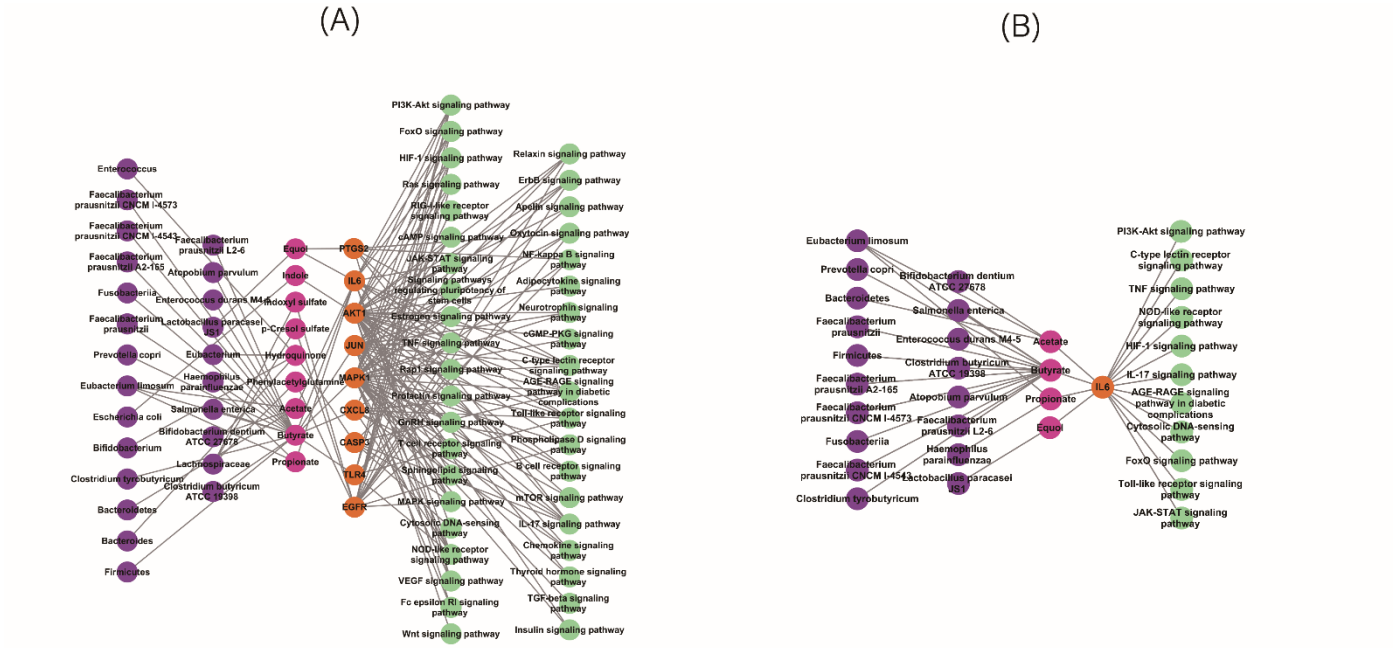

Figure 6. MMTS network. Purple circle: gut microbiota; Pink circle: metabolitered; Orange circle: target; Green circle: signaling pathway. (**A**) The overall MMTS network. (**B**) MMTS network of the core target IL6.

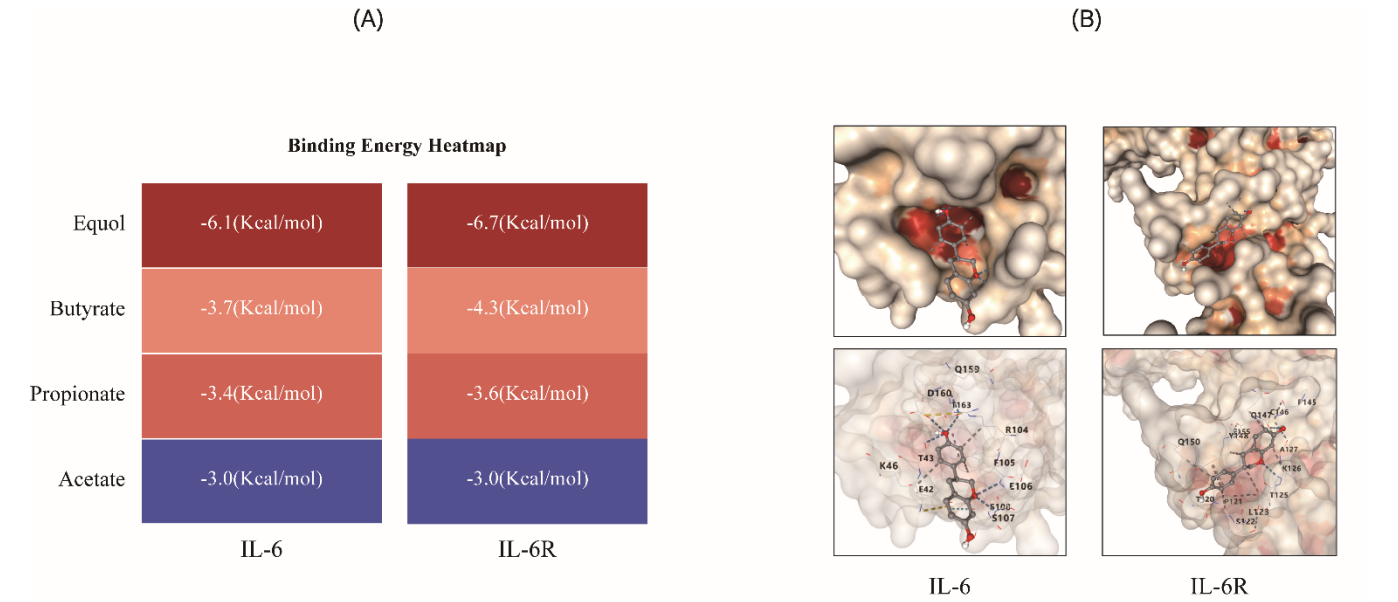

Figure 7. Equol-IL6 and Equol-IL6R complex on MDT. (**A**) Molecular docking result. (**B**) Equol-IL6 and Equol-IL6R molecular docking result.

3.6. Experimental Result

The CCK-8 viability assay showed that DMSO did not affect cell viability, while Equol significantly reduced cell viability at concentrations higher than 10^{-6} mol/mL (Figure 8A). The qPCR and WB results demonstrated that IL6 expression decreased significantly as the drug concentration increased. (Figure 8B).

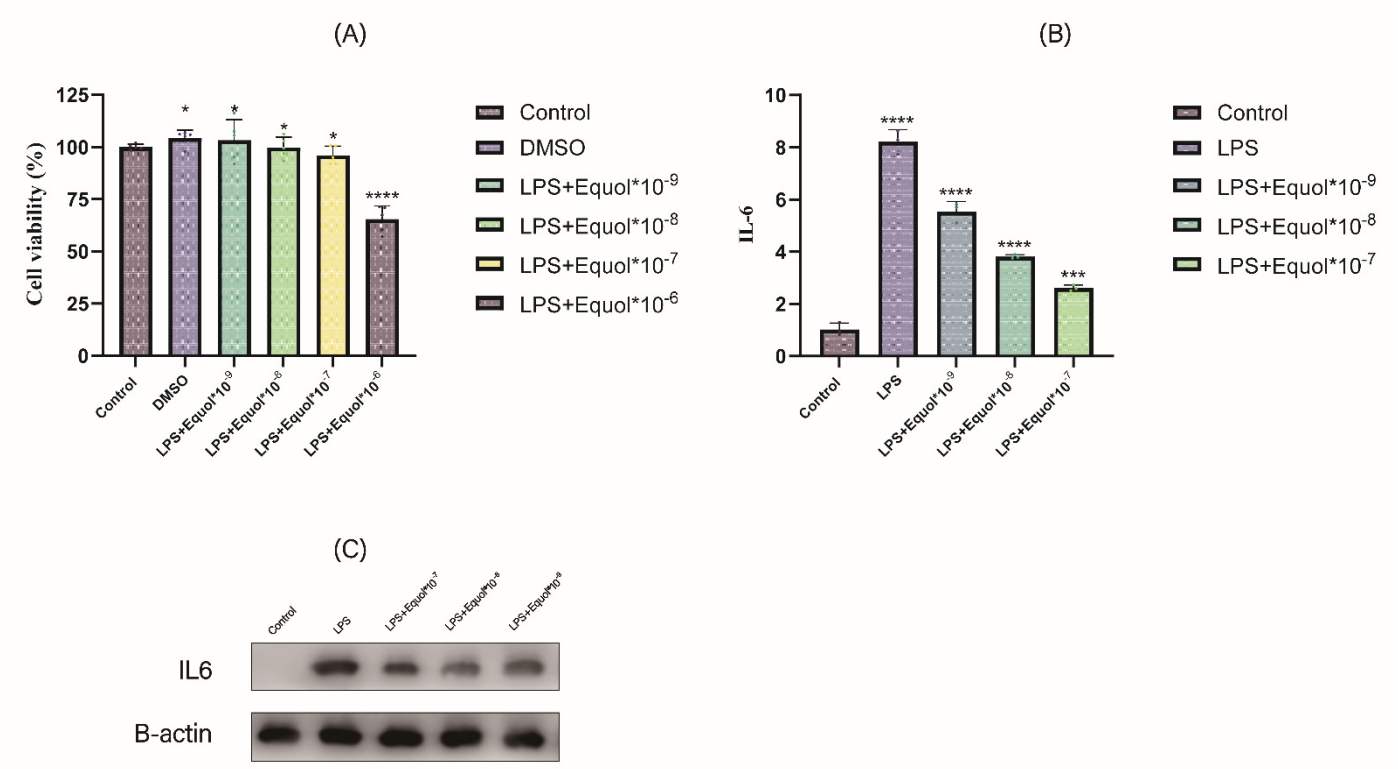

Figure 8. Experimental result. (**A**) Cell viability of THP-1 cells treated with different concentrations of Equol. (**B**,**C**) IL6 expression levels in THP-1 cells treated with Equol and LPS.* $p \leq 0.05$; *** $p \leq 0.001$; **** $p \leq 0.0001$.

4. Discussion

Research has shown the significant influence of gut microbiota on different organs, such as the lungs. The complex relationship between gut microbiota and lung function, known as the 'gut-lung axis,' is crucial for immune response and regulation [29].

Studies have shown that quercetin can influence the progression of pulmonary fibrosis [30], and quercetin is a flavonoid metabolite found in the gut. However, it remains unclear whether other metabolites in the gut can also affect pulmonary fibrosis. In recent years, network pharmacology studies have been employed for diagnosing various diseases and identifying target substances. In this study, we constructed a Metabolite-Microbiota-Target-Signaling (MMTS) network using network pharmacology to explore the interactions between metabolites and the gut microbiota.

In the PPI (protein-protein interaction) network, we identified Interleukin-6(IL6) as the key target. In the MMTS network, we found that 9 metabolites related to IPF in intestinal microbial metabolites can be divided into 6 categories: short-chain fatty acids (3 compounds), indoles (1 compound), sulfatolates (2 compounds), quinones (1 compound), organic acids (1 compound), and flavonoids (1 kind). There were four kinds of intestinal metabolites that could affect IL6, which were divided into short-chain fatty acids and flavonoids according to structure.

Butyrate can inhibit TGF-β1-induced alveolar myoblast differentiation and regulate energy metabolism in these short-chain fatty acids. However, no studies have definitively shown the relationship between the other two short-chain fatty acids and IPF [31].

Molecular docking is a computational method that can be used to predict the binding of small-molecule ligands to macromolecular proteins. [32]

Molecular docking experiments showed that Equol has high molecular activity, can affect IL6 and IL6R, and binds to IL6 and IL6R more stably than the other three compounds [33]. At the same time, *in vitro* cellular experiments also demonstrate that Equol can effectively influence the production of IL-6.

IL-6 is a multifunctional cytokine involved in various biological processes, including inflammation, immune response, and hematopoiesis [34]. In the early stages of pulmonary fibrosis, IL-6 plays a crucial role by promoting inflammation and facilitating the recruitment of inflammatory cells. This cytokine can exacerbate lung inflammation, leading to further tissue damage and fibrosis [35].

Importantly, IL-6 is essential for the inflammatory phase and the transition to a reparative environment during the resolution of wound healing. However, if the switch to the proliferative phase is uncontrolled, it can ultimately lead to fibrosis. Elevated levels of IL-6 have been correlated with decreased lung function in patients, underscoring its significance in the pathogenesis of pulmonary fibrosis [36].

Lactobacillus paracasei JS1, a strain of probiotic bacteria commonly found in fermented foods and the human gut, has been shown to promote gut health and modulate immune function. This probiotic plays an important role in maintaining the balance of gut microbiota and has potential health benefits through its anti-inflammatory and immune-boosting properties.

Equol, the final metabolite of soybean isoflavones metabolized by *Lactobacillus paracasei* JS1 in the human gut. The biological activity of soy isoflavones is enhanced by equol, which has been found to exhibit higher biological efficacy compared to soy isoflavones. Equol can boost the antioxidant defense system through multiple mechanisms, as evidenced by research showing its ability to reduce the expression of pro-inflammatory cytokines, and lower oxidative stress [23].

The potential synergistic effects of *Lactobacillus paracasei* JS1 and equol on pulmonary fibrosis outcomes provide an intriguing area for further investigation.

In this study, we constructed a microbiota-metabolite-target-signaling pathway (MMTS) network from a systematic perspective via a Network Pharmacology Study to elucidate the key microbiomes, signaling pathways, important targets, and metabolites that may influence idiopathic pulmonary fibrosis (IPF). This network provides a novel perspective for understanding the complex interactions between microbial communities and their hosts. we specifically focused on Equol, a metabolite produced by *Lactobacillus paracasei* JS1. Through analysis of the MMTS network, we discovered that Equol can modulate IL-6, a critical target in pulmonary fibrosis. This finding offers new insights into the pathogenesis of IPF. Furthermore, the construction of the MMTS network aids in uncovering gut microbiome metabolites that may influence the development of IPF, providing new directions and insights for future research.

Supplementary Materials

The following supporting information can be found at: https://www.sciepublish.com/article/pii/329. Table S1: Gut microbiota data from the gutMGene database. Table S2: The number of 1256 targets from SEA; the number of 948 targets from STP; the number of 668 overlapping targets between SEA and STP; the number of 1130 targets related to IPF targets; the number of 118 targets between two databases (SEA and STP) and IPF targets; the number of 20 final targets.

Statement of the Use of Generative AI and AI-Assisted Technologies in the Writing Process

During the preparation of this manuscript, the authors used ChatGPT (OpenAI) for grammar correction and language refinement. The authors carefully reviewed and edited all AI-assisted content to ensure its accuracy, originality, and integrity, and they take full responsibility for the final version of the published article.

Acknowledgements

Supported by The High Performance Computing Center of Henan Normal University. Ministry of Science and Technology, PR China, 2019YFE0119500, State Innovation Base for Pulmonary Fibrosis (111 Project), and Henan Project of Science and Technology, 212102310894, 222102310711, 232102310067, and 232102521025, Xinxiang Major Project 21ZD002.

Author Contributions

Y.G., L.W. designed the experiment; Z.L. performed experiments and completed the manuscript; Z.Z., J.W. and. provided data analysis; Y.Y., M.Z.,Y.G. provided literature revision and final editing of the manuscript.

Ethics Statement

Not applicable.

Informed Consent Statement

Not applicable.

Data Availability Statement

Data available within the article or its supplementary materials. The authors confirm that the data supporting the findings of this study are available within the article and its supplementary materials.

Funding

Ministry of Science and Technology, PR China grant 2019YFE0119500; Key R&D Program of Henan province grant 231111310400; Zhongyuan scholar 244000510009; Henan Project of Science and Technology grants 232102521025, and GZS2023008.

Declaration of Competing Interest

The authors declare no competing interests.

References

1. Sheu CC, Chang WA, Tsai MJ, Liao SH, Chong IW, Kuo PL. Bioinformatic analysis of next-generation sequencing data to identify dysregulated genes in fibroblasts of idiopathic pulmonary fibrosis. *Int. J. Mol. Med.* **2019**, *43*, 1643–1656.
2. Cao MS, Sheng J, Wang TZ, Qiu XH, Wang DM, Wang Y, et al. Acute exacerbation of idiopathic pulmonary fibrosis: Usual interstitial pneumonitis vs. possible usual interstitial pneumonitis pattern. *Chin. Med. J.* **2019**, *132*, 2177–2184.
3. Chunxi L, Haiyue L, Yanxia L, Jianbing P, Jin S. The Gut Microbiota and Respiratory Diseases: New Evidence. *J. Immunol. Res.* **2020**, *1*, 2340670.
4. Yanai H, Fraifeld VE. The role of cellular senescence in aging through the prism of Koch-like criteria. *Ageing Res. Rev*. **2018**, *41*, 18–33.
5. She YX, Yu QY, Tang XX. Role of interleukins in the pathogenesis of pulmonary fibrosis. *Cell Death Discov.* **2021**, *7*, 52.
6. Sgalla G, Iovene B, Calvello M, Ori M, Varone F, Richeldi L. Idiopathic pulmonary fibrosis: Pathogenesis and management. *Respir. Res.* **2018**, *19*, 32.
7. Toren D, Yanai H, Abu Taha R, Bunu G, Ursu E, Ziesche R, et al. Systems biology analysis of lung fibrosis-related genes in the bleomycin mouse model. *Sci. Rep.* **2021**, *11*, 19269.
8. Desai O, Winkler J, Minasyan M, Herzog EL. The Role of Immune and Inflammatory Cells in Idiopathic Pulmonary Fibrosis. *Front. Med.* **2018**, *5*, 43.
9. Deng KM, Yang XS, Luo Q, She YX, Yu QY, Tang XX. Deleterious Role of Th9 Cells in Pulmonary Fibrosis. *Cells* **2021**, *10*, 3209.
10. Ouyang W, Rutz S, Crellin NK, Valdez PA, Hymowitz SG. Regulation and functions of the IL-10 family of cytokines in inflammation and disease. *Annu. Rev. Immunol.* **2011**, *29*, 71–109.
11. Andoh A, Nishida A. Pro- and anti-inflammatory roles of interleukin (IL)-33, IL-36, and IL-38 in inflammatory bowel disease. *J. Gastroenterol.* **2023**, *58*, 69–78.
12. Ge Y, Huang M, Zhu XM, Yao YM. Biological functions and clinical implications of interleukin-34 in inflammatory diseases. *Adv. Protein Chem. Struct. Biol.* **2020**, *119*, 39–63.
13. Wang J, Kurilshikov A, Radjabzadeh D, Turpin W, Croitoru K, Bonder MJ, et al. Meta-analysis of human genome-microbiome association studies: The MiBioGen consortium initiative. *Microbiome* **2018**, *6*, 101.
14. Avelar-Barragan J, DeDecker L, Lu ZN, Coppedge B, Karnes WE, Whiteson KL. Distinct colon mucosa microbiomes associated with tubular adenomas and serrated polyps. *NPJ Biofilms Microbiomes* **2022**, *8*, 69.
15. Shi N, Li N, Duan X, Niu H. Interaction between the gut microbiome and mucosal immune system. *Mil. Med. Res.* **2017**, *4*, 14.
16. Zhan S, Li N, Liu C, Mao R, Wu D, Li T, et al. Intestinal Fibrosis and Gut Microbiota: Clues From Other Organs. *Front. Microbiol.* **2021**, *12*, 694967.
17. King TE, Pardo A, Selman M. Idiopathic pulmonary fibrosis. *Lancet* **2011**, *378*, 1949–1961.
18. Zhang X, Veliky CV, Birru RL, Barinas-Mitchell E, Magnani JW, Sekikawa A. Potential Protective Effects of Equol (Soy Isoflavone Metabolite) on Coronary Heart Diseases-From Molecular Mechanisms to Studies in Humans. *Nutrients* **2021**, *13*, 3739.
19. Ashley SL, Sjoding MW, Popova AP, Cui TX, Hoostal MJ, Schmidt TM, et al. Lung and gut microbiota are altered by hyperoxia and contribute to oxygen-induced lung injury in mice. *Sci. Transl. Med.* **2020**, *12*, eaau9959.
20. Yang J, Shi X, Gao R, Fan L, Chen R, Cao Y, et al. Polydatin alleviates bleomycin-induced pulmonary fibrosis and alters the

gut microbiota in a mouse model. *J. Cell Mol. Med*. **2023**, *27*, 3717–3728.
21. Gurczynski SJ, Lipinski JH, Strauss J, Alam S, Huffnagle GB, Ranjan P, et al. Horizontal transmission of gut microbiota attenuates mortality in lung fibrosis. *JCI Insight* **2023**, *9*, e164572.
22. Moriyama M, Hashimoto A, Satoh H, Kawabe K, Ogawa M, Takano K, et al. S-Equol, a Major Isoflavone from Soybean, Inhibits Nitric Oxide Production in Lipopolysaccharide-Stimulated Rat Astrocytes Partially via the GPR30-Mediated Pathway. *Int. J. Inflam.* **2018**, *1*, 8496973.
23. Subedi L, Ji E, Shin D, Jin J, Yeo JH, Kim SY. Equol, a Dietary Daidzein Gut Metabolite Attenuates Microglial Activation and Potentiates Neuroprotection *In Vitro*. *Nutrients* **2017**, *9*, 207.
24. Lin IC, Yamashita S, Murata M, Kumazoe M, Tachibana H. Equol suppresses inflammatory response and bone erosion due to rheumatoid arthritis in mice. *J. Nutr. Biochem.* **2016**, *32*, 101–106.
25. Budden KF, Gellatly SL, Wood DL, Cooper MA, Morrison M, Hugenholtz P, et al. Emerging pathogenic links between microbiota and the gut-lung axis. *Nat. Rev. Microbiol.* **2017**, *15*, 55–63.
26. Oh KK, Gupta H, Min BH, Ganesan R, Sharma SP, Won SM, et al. Elucidation of Prebiotics, Probiotics, Postbiotics, and Target from Gut Microbiota to Alleviate Obesity via Network Pharmacology Study. *Cells* **2022**, *11*, 2903.
27. Piñero J, Saüch J, Sanz F, Furlong LI. The DisGeNET cytoscape app: Exploring and visualizing disease genomics data. *Comput. Struct. Biotechnol. J.* **2021**, *19*, 2960–2967.
28. Amberger JS, Bocchini CA, Scott AF, Hamosh A. OMIM.org: Leveraging knowledge across phenotype-gene relationships. *Nucleic Acids Res.* **2019**, *47*, D1038–D1043.
29. Wypych TP, Wickramasinghe LC, Marsland BJ. The influence of the microbiome on respiratory health. *Nat. Immunol.* **2019**, *20*, 1279–1292.
30. Wu W, Wu X, Qiu L, Wan R, Zhu X, Chen S, et al. Quercetin influences intestinal dysbacteriosis and delays alveolar epithelial cell senescence by regulating PTEN/PI3K/AKT signaling in pulmonary fibrosis. *Naunyn Schmiedebergs Arch. Pharmacol.* **2024**, *397*, 4809–4822.
31. Lee HY, Nam S, Kim MJ, Kim SJ, Back SH, Yoo HJ. Butyrate Prevents TGF-β1-Induced Alveolar Myofibroblast Differentiation and Modulates Energy Metabolism. *Metabolites* **2021**, *11*, 258.
32. Zhang Y, Li X, Yu Q, Lv X, Li C, Wang L, et al. Using network pharmacology to discover potential drugs for hypertrophic scars. *Br. J. Dermatol.* **2024**, *191*, 592–604.
33. Mayo B, Vázquez L, Flórez AB. Equol: A Bacterial Metabolite from The Daidzein Isoflavone and Its Presumed Beneficial Health Effects. *Nutrients* **2019**, *11*, 2231.
34. Tanaka T, Narazaki M, Kishimoto T. Interleukin (IL-6) Immunotherapy. *Cold Spring Harb. Perspect. Biol.* **2018**, *10*, a028456.
35. Epstein SG, Brook E, Bardenstein-Wald B, Shitrit D. TGF-β pathway activation by idiopathic pulmonary fibrosis (IPF) fibroblast derived soluble factors is mediated by IL-6 trans-signaling. *Respir. Res.* **2020**, *21*, 56.
36. Johnson BZ, Stevenson AW, Prêle CM, Fear MW, Wood FM. The Role of IL-6 in Skin Fibrosis and Cutaneous Wound Healing. *Biomedicines* **2020**, *8*, 101.